Article

Disentangling the Photophysics of DNA-Stabilized Silver Nanocluster Emitters

Matías Berdakin,[†] Martín Taccone,[‡] Kranz J. Julian,[§] Gustavo Pino,[‡] and Cristián G. Sánchez*,[†]

[†]INFIQC (UNC-CONICET), Dpto. de Matemática y Física, Fac. de Ciencias Químicas, and [‡]INFIQC (UNC-CONICET), Dpto. de Fisicoquímica, Fac. de Ciencias Químicas, Centro Laser de Ciencias Moleculares, Universidad Nacional de Córdoba, Ciudad Universitaria, Pabellón Argentina, 5000 Córdoba, Argentina

[§]Department of Chemistry, Karlsruhe Institute of Technology, Kaiserstrasse 12, 76131 Karlsruhe, Germany

S *Supporting Information*

ABSTRACT: It has been already established that DNA−silver fluorophores present two intense absorption bands, one in the visible and the other in the UV spectral region, and that the excitation of both bands produces a common fluorescence signal. Nevertheless, the detailed mechanism responsible for this coupling is still elusive. In this context, our work is a significant leap forward in this goal by providing a dynamic picture of the excitation and the processes that take place upon light absorption in these systems using a time-dependent density functional tight-binding approach. In the present work, we explore the electronic coupling mechanism in a cluster composed of a double string of deoxypolycytosine with six bases and a rod of six Ag atoms.
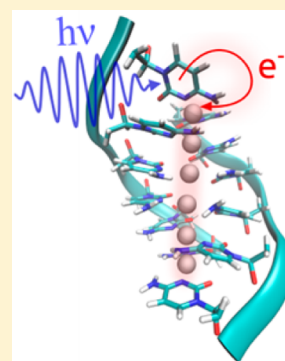
■ INTRODUCTION

In the past years, natural and artificial DNA molecules have been of great interest because of their potential applications in biological and material science.[1−5] The incorporation of metal-mediated base pairing has proven to be a suitable and powerful tool for the potential development of artificial DNA-based devices.[6−8] In this sense, one interesting application is the production of highly fluorescent and tunable hybrid DNA−Ag$_n$ clusters. The optical properties of these hybrid systems (e.g., high fluorescence yield and absorption/emission wavelength tuning) are strongly dependent on the nucleobase sequence [the presence of cytosine (C) or guanine (G) is specially needed for fluorescent clusters[9−12]], cluster size,[13] pH,[14] temperature,[15] etc. These photophysical properties of silver clusters have led to the creation of a new generation of small and biocompatible fluorophores as biological labels that exceed the commonly used semiconductor quantum dots and organic dyes with regard to fluorescence quantum yield, photostability, and biocompatibility, due to the low toxicity and very small size of the Ag$_n$ clusters.[9,16] For more information about these novel systems, readers are recommended to refer to recent reviews on the topic.[9,17−22]

The rational design of DNA−Ag$_n$ clusters for such applications requires a full understanding of how metal−base interactions determine their optical properties, and in this context, detailed experimental and theoretical results are highly desirable. Our work is a significant leap in this sense by providing a dynamic picture of excitation and the processes that take place upon light absorption in these systems using a time-dependent density functional tight-binding approach.

A substantial contribution to the understanding of how a metal−base interaction determines cluster structure and spectroscopical response was recently provided by Gwinn and colleagues.[23] By means of purification and spectral character-ization of size-selected DNA−Ag$_n$ clusters by HPLC coupled to ESI-MS. In this work, the authors provide strong experimental and theoretical evidence pointing to rodlike Ag$_n$ clusters produced between and along the DNA strands that are anchored by Ag$^+$ cations acting as a bridge between the DNA bases and the rod. Besides, the number n of Ag atoms forming the rod has been related with its color.[23] In subsequent reports, the idea of a rod-shaped cluster was successfully employed to simulate experimental results. The main idea was to relate the neutral core of the rods with absorption and circular dichroism spectroscopy.[23−27]

Another interesting property of hybrid DNA−Ag$_n$ clusters is the fact that they have two intense absorption bands. One of these bands, in the visible range, is tunable via DNA base sequence and/or the number of Ag atoms and the other, in the UV spectral region, is common to all of them, regardless of the position of the visible band.[9,12,14,28] The UV excitation band is located in the spectral region where the isolated bases and DNA strands absorb (260−270 nm). It was previously suggested that this peak could be due to excitation to higher-lying states;[28] however, recent evidence indicates that the UV absorption band corresponds to excitation of the nucleobases.[12]

A

On the other hand, in a bottom-up approach, recent results from laser spectroscopy of gas-phase (cytosine)$_2$Ag$^+$ clusters confirmed that the band at 286 nm is due to a $\pi^* \leftarrow \pi$ transition within the cytosine moiety. In the same study, an enhancement was shown of at least 3 orders of magnitude in the excited state lifetime of the (cytosine)$_2$H$^+$ cluster when H$^+$ is replaced by Ag$^+$, a fact which was attributed to the energy of the nπ^* state involving the d orbital of Ag$^+$.[29]

Interestingly, the excitation of the common UV band leads to the same fluorescence spectrum as in the case of excitation of the tunable visible band,[12] suggesting that the electronic coupling between the DNA excited state and the Ag$_n$ rodlike cluster might be strong and ultrafast. This is a useful property for different applications of these clusters, since it allows one to use a single UV excitation source for all cases, to obtain tunable fluorescence spectra. Recently, a charge transfer (CT) process from cytosine to Ag$^+$ was observed upon UV excitation of the simplest cytosine–Ag$^+$ complex in the gas phase, which could be the foundation for the electronic coupling process between the two moieties.[30] Despite its importance in the rational design of highly fluorescent DNA–Ag$_n$ clusters, the detailed mechanism responsible for this coupling is still elusive.

In this context, within the present work we explore the electronic coupling mechanism in a system composed by a double string of deoxypolycytosine with six bases (hereafter dpC$_6$) and a rod of six Ag atoms. The choice we made for the geometric arrangement of the neutral silver atoms in the complex is founded on two main reasons: (1) The vast amount of experimental and theoretical data provided by Gwinn,[23] have proven that the relation between the state of charge and the optical properties of this cluster is not trivial. Taking this into account, the present work attempts to be the first step in the construction of a model of growing complexity that allows the study of the optical properties of silver–DNA emitters, and the choice of the neutral clusters as a starting point is related to a bottom-up complexity approach. In this sense, it is worth noting that Gwinn and co-workers[23,24] and Aikens and co-workers[25−27] have successfully interpreted experimental results supported by the calculation of the absorbance spectra and circular dichroism signals of the neutral wires of silver atoms. (2) In their original report, Dickson and colleagues[14] show that the synthesis of fluorescent clusters using silver nitrate and sodium borohydride as the reducing agent, with 12 cytosine simple helix DNA strands, led to the formation of a mixture of reduced and partially oxidized emitters. Recent research has turn its attention to the study of the optical properties of partially charged clusters,[13,23,24,31] assisted by the implementation of HPLC coupled with high-resolution MS.[23] This experimental setup provides the most detailed description of the optical properties of partially and totally charged clusters available to date regarding the structure and charge effects on the photophysical properties of this kind of cluster.

On the other side, the election of the size of the model system employed in this report was mainly done in order to establish a balance between the need to account for the more realistic system possible while the computational cost of the simulation was kept affordable. This report is the first step in a study of growing complexity on the optical properties of DNA-protected silver emitters. Another important reason to limit the size of the system to six Ag atoms is that the cluster containing six Ag ions is the biggest completely ionic system studied experimentally.[23] The neutral six Ag atom cluster constitutes a promising system to evaluate the effect of charge, and therefore, the election of the system employed in this work would enable us in the future to make a straightforward comparison with a realistic completely ionic cluster.

Regarding the selection of the structural models studied in the present work, we believe that an extensive amount of experimental information, contrasted with computational simulations, reinforce the idea of a structure consisting of a rod extended between and along the DNA double helix.[23,32,33] There is also evidence from the gas and liquid phase that points to the fact that the silver cation in the C−Ag+C mismatch is placed between the N3 of both cytosines,[33−36] and the main structural features (with regard to the existence of the rod-shaped cluster) are not modified after chemical reduction;[24] however, readers have to be alert to the fact that so far there has been no direct determination of the structure of DNA−silver fluorophores. In particular, the details of the metal−ligand binding are not well established.

■ COMPUTATIONAL METHODS

The dpC$_6$−Ag$_6$ cluster was generated by the Nucleic Acid Builder (NAB)[37] together with the Visual Molecular Dynamics (VMD)[38] visualization program. Simulations of a solvated and charge-neutralized dpC$_6$−Ag$_6$ cluster were performed in an *NVT* assembly, using a 60-Å-side cubic box with explicit water. Molecular dynamics were carried out using the large-scale atomic−molecular massively parallel simulator (LAMMPS).[39] The Charmm force field[40,41] was used to describe DNA interactions, while silver−silver and silver−DNA bonds, angles, and dihedrals were approximated using Ag$_n$−pyridine[42] and Zn-containing model system[43] parameters. Nonbonded parameters were taken from the work of Vercauteren and co-workers.[44] These parameters have been been used in the past to model successfully the structural, energetic, and dynamic properties of few-atom silver clusters embedded in DNA strands by Vercauteren and co-workers[44] and to provide structural models also based on molecular dynamics simulations for more complex structures than the one studied in our work by Gwinn.[13] First, an energy minimization was performed, followed by a 10 ns run at a temperature of 300 K. An ensemble of 20 structures was randomly selected from the 10 ns run after the stabilization of the thermodynamics properties during the molecular dynamics, and all the results were calculated as the ensemble average of this manifold of structures. Besides including the effect of thermal noise in the DNA backbone and wire, this strategy allows one to account for the fluctuations of structural parameters such as Ag−Ag and Ag−N bond distances and Ag−Ag−Ag and N−Ag−N angles in the photophysical properties studied within this report.

The methodology employed to study electronic properties applied in this work has been widely described[45−47] and is based on the time propagation of the one electron density matrix under the influence of external time-varying electric fields. The electronic dynamics is fully described, taking into account to all orders the influence of the external field. The dynamic observables that are shown in this work stem from the dynamics of the whole single particle density matrix evolving in the external field, allowing for arbitrary mixing of excited states that are close in energy. This methodology allows one to obtain optical information on the system both within and outside the linear response regime. The electronic structure is obtained from a density functional theory based tight-binding (DFTB) Hamiltonian.[48] The DFTB+ code,[49] which implements self-consistent DFTB, was used to model the electronic structure of

the cluster system in its ground state, using the mio 1.1 DFTB parameter sets.[48,50] The standard mio parameter set was extended to include Ag by running the required DFT calculations for the generation of the matrix elements with all the rest of the mio set atoms setting all parameters (compression radii, basis set, etc.) as used in the generation of the mio set. The new electronic parameters between Ag and all other elements in the mio set are therefore fully consistent. These parameters are available from the authors upon request. Parameters for Ag were obtained from PBE calculations, with the zeroth-order regular approximation employed and DFTB compression radii of r_{dens} = 14 Å for the density and r_{wf} = 3.75 Å for the wave function. Optical absorption spectra are obtained by introducing an initial perturbation in the shape of a Dirac delta pulse to the initial ground-state density matrix.[46] After pulse application, the evolution of the density matrix can be calculated by time integration of its equation of motion. In the linear response regime, the absorption spectrum can be obtained from deconvolution of the dipole moment signal from the excitation waveform after a Fourier transform. In order to gain insight into the nature of the electronic transitions that are observed in the spectrum, a perturbation consisting in a sinusoidal time-dependent electric field is tuned with the absorption maximum of the band of interest with the polarization direction of the field chosen to match the transition dipole moment vector direction. Under these irradiation conditions, the population of each state (i.e., the ones that are populated and the ones that are being depopulated because of the irradiation) can be straightforwardly obtained from the density matrix as a function of time, as well as the charge of each atom of the system. The details of the procedure employed have been described elsewhere.[45,47,51,52]

RESULTS AND DISCUSSION

For this study two model structures were considered. First, a reductionist approach was pursued, and a structure without the phosphate and ribose backbone was generated. For this purpose the cisoid C−Ag−C metal-mediated base pair (C_2Ag) was reproduced following the structural features of a DNA double helix, namely, base-to-base distance and base pair rotation. Figure 1a shows the obtained $(C_2Ag)_6$ structure built after six replications of the metal-mediated base pair unit. The second structure employed in this work seeks to account for the effect of the backbone and the structural disorder on the spectroscopy and photophysics of DNA−Ag. For this purpose, the complete structure of the $(dpC_6)_2Ag_6$ system was explored by means of an *NVT* molecular dynamics simulation of the system embedded in solvent and counterions. An ensemble of 20 structure was randomly selected from the 10 ns run after the stabilization of the thermodynamics properties during the molecular dynamics, and all the results were calculated as the ensemble average of this manifold of structures (for details see the Computational Methods section). Figure 1b shows a representative geometry obtained for $(dpC_6)_2Ag_6$.

The electronic structure of $(C_2Ag)_6$ and $(dpC_6)_2Ag_6$ were analyzed through the calculation of their density of states (DOS) shown in Figure 2, parts a and b, respectively. In black, red, and blue lines, the total DOS and the projected DOS (PDOS) for the DNA and Ag moieties are shown, respectively.

A close analysis of the DOS and the PDOS obtained for $(C_2Ag)_6$ reveals that four clearly distinguished feature zones can be established in the electronic structure. For the sake of clarity
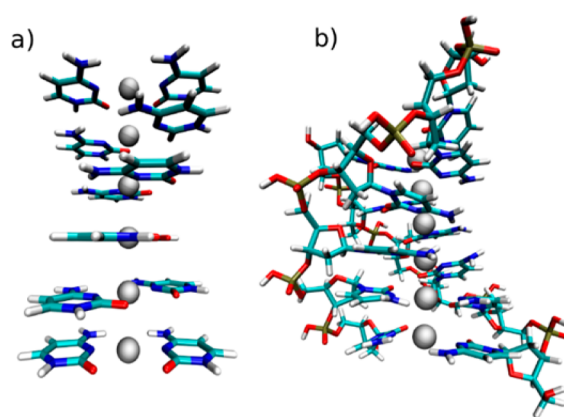

Figure 1. (a) Reductionist approach of the $(dpC_6)_2Ag_6$ cluster. The geometry was obtained by the replication of the C−Ag−C mismatch, holding up the structural parameters of a B-DNA double helix. The replication index is 6, giving rise to the $(C_2Ag)_6$ structure. (b) Representative structure, obtained from molecular dynamics simulation, of $(dpC_6)_2Ag_6$ considering the complete backbone of the DNA helix. For details please refer to Computational Methods section.
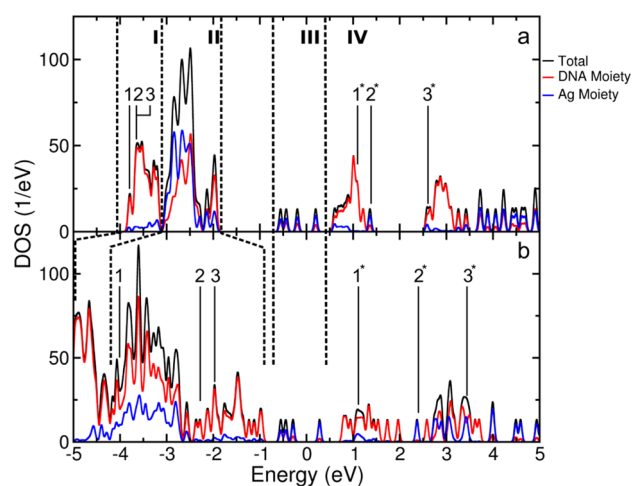

Figure 2. Electronic structure of $(C_2Ag)_6$ (a, upper panel) and $(dpC_6)_2Ag_6$ (b, lower panel), as represented by their densities of states. Black, red, and blue lines represent the total DOS and the PDOS obtained for DNA and Ag moieties, respectively.

in Figure 2, these four zones are highlighted with roman numerals and vertical dotted lines. The first one (I) consist of a manifold of states mainly generated by a large contribution of states coming from the DNA moiety (by DNA moiety we refer in all cases to all non-silver atoms) with an almost negligible contribution of the Ag moiety. On different grounds, the second feature zone (II) consists of a broad manifold where a significant mixture of states from DNA and Ag occurs. As energy increases, the contribution of the Ag moiety decreases until the DNA contribution turns dominant again. The third feature zone (III) occurs near the Fermi energy and consists of a series of four narrow groups of states, three of which fall at slightly lower energy than the Fermi level and a fourth one which falls above it. One important characteristic to highlight about zone (III) is that states within this zone, which include the HOMO and LUMO orbitals of the structure, are well-separated in energy from the other manifolds. In the fourth feature zone (IV), several manifolds of states occur, and an

alternation in the preponderance of the contribution between the DNA states and the silver moiety can be observed.

As a validation of the reductionist approach to properly represent the electronic structure of the system, the comparison between the results obtained for both structures considered here reveals that the presence of the DNA backbone does not significantly modify the differentiation of the main feature zones distinguished for the model $(C_2Ag)_6$ structure. In particular, the group of states close to the Fermi energy are virtually unmodified. The most important difference that can be observed for the $(dpC_6)_2Ag_6$ is that the second feature spans over a wider energy range, but the general descriptions of the four feature zones stand.

Toward the study of the spectroscopy and photophysics of DNA−Ag hybrid systems, the absorbance spectra of the structures considered here were calculated according to the methodology described in the Computational Method section. In panels a and b of Figure 3, the obtained spectra of $(C_2Ag)_6$ and $(dpC_6)_2Ag_6$, respectively, are shown in black lines.
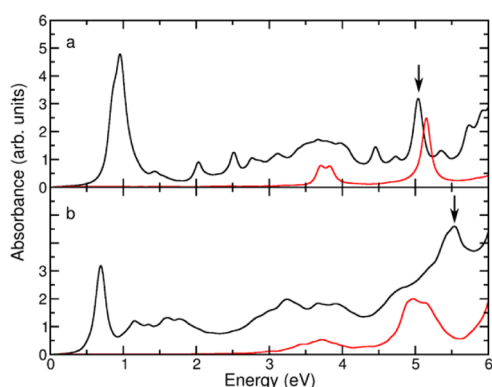

Figure 3. Black lines show the calculated absorption spectra of (a) $(C_2Ag)_6$ and (b) $(dpC_6)_2Ag_6$. Red lines show the absorption spectra of the DNA moieties of each structure. The excitation energies employed to perturb the systems in each case are indicated with arrows.

The corresponding absorption spectra of the isolated DNA moieties forming each structure are shown in red lines. Several important points from Figure 3 are worth highlighting. First, the calculated spectrum of both DNA moieties, with and without the presence of the backbone, present an intense absorption band around 5 eV. This is in qualitative agreement with experimental and theoretical results that have shown that the absorption spectrum of DNA presents an intense band in the UV region around 4.5−5.0 eV, commonly attributed to the $\pi\pi*$ transition of the DNA bases,[12] and a second, low intensity band around 3.5−4.0 eV, which is usually not experimentally observed.[53,54] Moreover, ample evidence exists showing that after the metallic nanocluster synthesis, the energy of the UV absorption band does not suffer major shifts, and new bands appear at the visible region of the spectrum.[12,23,55] As can be seen in Figure 3a, the results obtained from computational simulations are in agreement with this experimental observation, as the UV band suffers only a small shift when the complete cluster structure is considered. The same is true for the case of $(dpC_6)_2Ag_6$. Also, Figure 3a,b shows that for $(C_2Ag)_6$ and $(dpC_6)_2Ag_6$ an intense absorption band appears at low energies, as described experimentally,[23] and the energy of this absorption band is in agreement with that predicted from TDDFT for naked wires employed for the characterization of

the UV and circular dichroism signals.[23−27] It is important to note that the absorption bands observed in Figure 3 are broadened with respect to the ones experimentally observed.[23] These spectral changes can be explained by a combination of causes, such as the broadening caused by small hybridization with states coming from the DNA backbone and the lack of a complete environment and charging of the backbone. Also the state of charge of the silver wire represents another source of disagreement with the experimental results.

The nature of the UV absorption band was studied by electronic dynamics, as this methodology has proved to provide a deep understanding of the electronic excitation through the calculation of relevant time-dependent properties like molecular orbital population and time-dependent charges.[45,51,52]

A sinusoidal time-dependent electric field, tuned with the absorption maximum in the UV region of each spectra, was applied to both $(C_2Ag)_6$ and $(dpC_6)_2Ag_6$. The polarization direction of the field was chosen to match the transition dipole moment at that energy for each of the structures.[47] For $(C_2Ag)_6$, the energy was tuned with the peak at 5.04 eV (pointed out with arrow in Figure 3a), and for the $(dpC_6)_2Ag_6$ system, the irradiation was tuned to match the corresponding energy maximum for each structure of the ensemble. Schematically, the position in the absorption spectra is shown with arrows in Figure 3b for the ensemble average.

The time-dependent molecular orbital population analysis allows one to determine which molecular orbitals are involved in the optical excitation. Orbitals populated and depopulated during light irradiation are shown in Figure 4, parts a and 4b, for $(C_2Ag)_6$ and $(dpC_6)_2Ag_6$, respectively, and the energies of their eigenvalues within the respective DOSs are depicted in Figure 1 with lines and numbers.
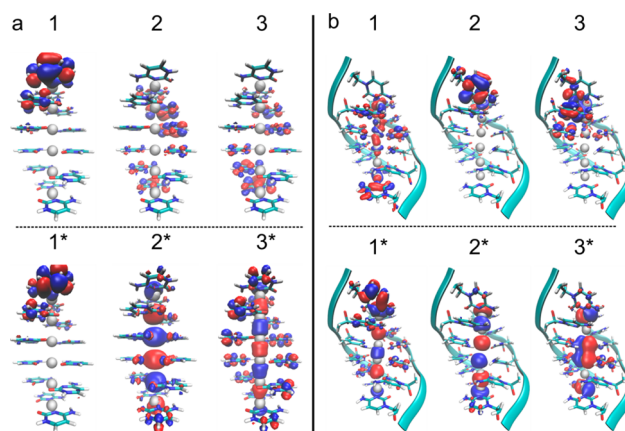

Figure 4. Populated and depopulated molecular orbitals during light irradiation. Panels a and b present the results obtained for $(C_2Ag)_6$ and $(dpC_6)_2Ag_6$, respectively. The depopulated orbitals are labeled with numbers (N), increasing with their corresponding energy. Populated orbitals are labeled with numbers $N*$.

In Figure 4a it can be observed that for the case of $(C_2Ag)_6$, the depopulated orbitals (1, 2, and 3) correspond to π orbitals of the DNA bases, and no contribution of Ag orbitals is observed. This is clearly visualized in Figure 2a, where it can be seen that these states form part of the feature zone I; therefore, they have a negligible contribution from Ag moiety states. The states that are populated during the light excitation are labeled 1*, 2*, and 3*; state 1* corresponds to a localized $\pi*$ state, that in Figure 2a is found in zone IV of the DOS, also with

negligible contribution of the Ag moiety. At first glance, this result can lead to the interpretation that the UV transition of the DNA−silver hybrid fluorophores corresponds to the pure $\pi\pi^*$ excitation of the DNA bases. Nevertheless, as can be seen from Figure 4a, orbitals 2* and 3* correspond to delocalized states, with a significant amount of charge transfer to the silver moiety. This is corroborated through Figure 2a, where it can be observed that orbitals 2* and 3* have a significant contribution from Ag states. In order to explore the charge dynamics during light irradiation, time-dependent Mulliken atomic charge changes with respect to the ground state charge (ΔCharge) in both moieties were calculated. Figure 5a shows as black and red lines the ΔCharge obtained for Ag and DNA moieties of $(C_2Ag)_6$, respectively.
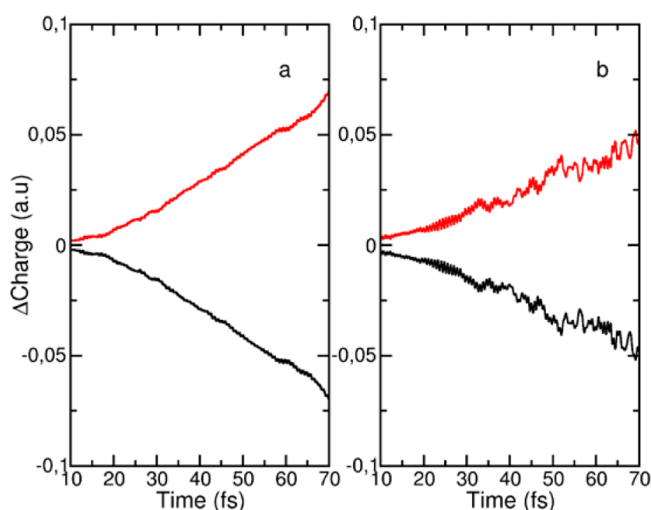

Figure 5. Time-dependent Mulliken atomic charges with respect to the ground state (ΔCharge). Panels a and b show the obtained results for $(C_2Ag)_6$ and $(dpC_6)_2Ag_6$, respectively. DNA and Ag moiety ΔCharge are shown as red and black lines, respectively.

As can be clearly observed, a net negative charge transfer from the DNA moiety to the Ag moiety occurs during light irradiation, despite of the fact that this is not a charge transfer excitation. This interesting finding indicates that the most relevant photophysical process induced upon UV excitation of the $(C_2Ag)_6$ structure involves a slower charge transfer process from DNA to Ag, and "slower" here is taken in the context of what would be a vertical excitation; the charge transfer is, indeed, ultrafast but comes out as a result of the evolution of the excited wave packet.

The general conclusions obtained for the model system $[(C_2Ag)_6]$ remain essentially unchanged when the structure with the complete backbone $[(dpC_6)_2Ag_6]$ is considered. In Figure 4b, the populated and depopulated molecular orbitals obtained from the analysis of the time-dependent molecular orbital population are shown. The depopulated orbitals are labeled with 1, 2, and 3. As can be observed in Figures 4b and 2b, all depopulated orbitals present some degree of mixing between states from both moieties. Orbitals 2 and 3 correspond to π cytosine orbitals, with a small and localized contribution of the d shell of the Ag moiety, and on the other hand, orbital 1 presents some delocalization through Ag atoms. The populated orbitals are labeled 1*, 2*, and 3*. Similar to the case of $(C_2Ag)_6$, orbital 1* presents a predominantly π^* character with a non-negligible contribution of delocalized Ag states, while

orbitals 2* and 3* have a majority of Ag contribution, delocalized through the moiety. Figure 5b shows the ΔCharge obtained for both moieties of $(dpC_6)_2Ag_6$ as a function of time. It can be clearly observed that neither the presence of the backbone nor the disorder of the structure preclude the charge transfer process.

It is worth noting that the UV absorption band obtained for dpC_6−Ag_6 is rather broad. Nevertheless, several irradiation energies taking into account the main peaks of the spectrum were employed, and the analyses of the time-dependent molecular orbital population and charges were reproduced in all cases, indicating that the processes observed are robust and present for the whole band. Variations of the mixing of states from both moieties in the ground state have been observed, but the charge transfer process occurs regardless of the excitation energy employed (see Figure S1, Supporting Information).

As a summary of the results presented so far, excitation of the UV bands of the complex causes promotion of electrons from states belonging to zone I (mainly cytosine π orbitals) into states of zone IV, having a contribution from Ag orbitals. Concomitantly, a charge transfer process occurs that transfers electrons from the bases into the Ag rod with a time scale of tens of femtoseconds. Taking into account that the excitation of the visible band of DNA−Ag has been attributed to the longitudinal transition of the rod-shaped Ag moiety,[23] the charge transfer process reported here can be of fundamental interest as a means to understand the common fluorescence observed when the UV and the visible absorption bands are excited. As can be seen in Figure 4a,b, orbitals populated during UV light irradiation present a large delocalization in the longitudinal axis and resemble significantly those reported to be involved in the HOMO−LUMO longitudinal transition of isolated monatomic silver wires.[27] Furthermore, when the excitation energy is tuned with the most intense low-lying absorption band (around 1 eV) of each structure, the population molecular orbital analysis shows that the populated orbitals consist of the 2* orbital, identified as one of the "receptors" of the electronic excitation when the UV absorptions band is excited, coupled with orbital 4* (see Figure S2, Supporting Information), which is indeed the LUMO of the isolated wire. It is our proposal that the charge transfer process described here provides a mechanistic pathway that explains the excitation interplay between both bands. No direct information on the fluorescence can be obtained from our calculations. However, electrons promoted to orbitals in region IV that trickle into excited Ag orbitals must find a relaxation pathway into the occupied, lower energy manifold. This pathway could be through the emission of phonons, by direct connection to the lower energy manifold (i.e., via conical intersections), or fluorescence. Our proposal is that the presence of virtually isolated Ag states in region III, clearly separated in energy and electronically decoupled from groups I where electrons are promoted from and IV where electrons are promoted to, provides a "gap" akin to those in semiconducting quantum dots. These states might be the key to unlock the cause for fluorescence in these systems. This would also provide a clue as to why fluorescent clusters are obtained when using Ag as the metal mediating base pairing; the energy tuning of this gap would be critical.

It is important to state some final notes on the robustness of the obtained results with respect to structural changes. The photophysical properties obtained for $(C_2Ag)_6$ and $(dpC_6)_2Ag_6$ are qualitatively similar because the origin of the charge transfer

process here described is grounded on the electronic landscape accounted in the DOS. The resemblance between parts a and b of Figure 1 indicates that the determinant factor in the conformation of the electronic structure of these systems is the interaction between the s, p, and d shells of Ag atoms and the states provided by the DNA bases, regardless of the presence of backbone states (which are expected to be at lower energies) and the structural disorder provided by this. As was stated in the Introduction, the choice of the structural models considered herein is based on the experimentally available information on the Ag−DNA interaction motif. Thus, as the authors chose model structures having this silver−base bonding, no further conclusions can be extracted from our simulation on the effect of this motif on the photophysical properties studied here. Also, it is important to emphasize that the purpose of the comparison between $(C_2Ag_6)_2$ and $(dpC_6)_2Ag_6$ is not to gain insight into the effect of the silver−base bonding but to provide information on whether the structural disorder provided by the DNA scaffold and thermal noise affects the photophysical properties and the charge transfer process explored in the present report.

Furthermore, we evaluated the effect of the cisoid/transoid isomerism of the glycosidic bond in the photophysical properties explored within this work. For this purpose, the model structure without the DNA backbone was employed and a double strand of transoid C−Ag−C mismatches was obtained in a similar manner as in the case of the cisoid structure. All the analysis were carried out, and the results are shown in Figure S3 (Supporting Information) in comparison with the already presented results for the cisoid isomer. From these results it can be seen that neither the electronic structure of the cluster nor the absorption spectra or the charge transfer process are quantitatively modified by the cisoid/transoid isomerism.

All the information stated in this section, together with the observation that the chemical bond is mainly driven by the overlap of d states of Ag and base states of DNA, can be another justification of the fact that there are just a few fluorescent hybrid systems obtained with DNA and other metals different than Ag.

CONCLUSIONS

In conclusion, in this work, the study of the spectroscopy and photophysics of the DNA−Ag hybrid system was pursued by means of electronic structure and quantum dynamics simulation of the systems under irradiation. The electronic structures of both structures considered here were studied through DOS and PDOS analysis. Similar features were observed for $(C_2Ag)_6$ and $(dpC_6)_2Ag_6$, among which the most important one reveals the presence of common feature zones, where the contribution of states from both moieties is reproduced, and the existence of a group of electronically decoupled, energy-isolated states separating manifold from which electrons are promoted from and to.

The simulation of the absorption spectra of both structures reproduces the features observed in experimental reports, i.e., a series of bands are observed, one in the UV spectral region near the absorption band of the DNA moiety and new bands in the visible region. The UV absorption band of the $(dpC_6)_2Ag_6$ structure is broadened and blue-shifted. This effect can be related to the lack of a complete environment and charge description of the system. Interestingly, the irradiation of the UV band shows that, in this transition, electrons are promoted from localized π states of the DNA to delocalized states of the

Ag moiety, leading to a net negative charge transfer during light irradiation. To the best of our knowledge, this finding reveals a new feature of the excited state dynamics of DNA−Ag hybrids systems and may set the grounds to understand the common fluorescence obtained when the UV and visible bands are excited. This can be explained by considering that the orbitals populated during UV irradiation, responsible for the charge transfer process, are common to those populated during visible irradiation.

■ ASSOCIATED CONTENT

ⓢ Supporting Information

The Supporting Information is available free of charge on the ACS Publications website at DOI: 10.1021/acs.jpcc.6b05363.

> Charge transfer process produced during laser irradiation at the broad UV band of the $(dpC_6)_2Ag_6$ structure and the populated orbitals after irradiation of the visible band of both systems $[(C_2Ag)_6$ and $(dpC_6)_2Ag_6]$ (Figures S1−S3) (PDF)

■ AUTHOR INFORMATION

Corresponding Author

*e-mail: cgsanchez@fcq.unc.edu.ar Telephone: +54 531 5353850 Ext. 55020.

Notes

The authors declare no competing financial interest.

■ REFERENCES

(1) Seeman, N. C. DNA in a Material World. *Nature* **2003**, *421* (6921), 427−431.

(2) Li, X.; Liu, D. R. DNA-Templated Organic Synthesis: Nature's Strategy for Controlling Chemical Reactivity Applied to Synthetic Molecules. *Angew. Chem., Int. Ed.* **2004**, *43*, 4848−4870.

(3) Lu, Y.; Liu, J. Functional DNA Nanotechnology: Emerging Applications of DNAzymes and Aptamers. *Curr. Opin. Biotechnol.* **2006**, *17*, 580−588.

(4) Feldkamp, U.; Niemeyer, C. M. Rational Design of DNA Nanoarchitectures. *Angew. Chem., Int. Ed.* **2006**, *45*, 1856−1876.

(5) Niemeyer, C. M.; Mirkin, C. A. *Nanobiotechnology: Concepts, Applications and Perspectives*; Wiley-VCH: Weinheim, Germany, 2004.

(6) Takezawa, Y.; Shionoya, M. Metal-Mediated DNA Base Pairing: Alternatives to Hydrogen-Bonded Watson-Crick Base Pairs. *Acc. Chem. Res.* **2012**, *45*, 2066−2076.

(7) Liu, S.; Clever, G. H.; Takezawa, Y.; Kaneko, M.; Tanaka, K.; Guo, X.; Shionoya, M. Direct Conductance Measurement of Individual Metallo-DNA Duplexes within Single-Molecule Break Junctions. *Angew. Chem., Int. Ed.* **2011**, *50*, 8886−8890.

(8) Park, K. S.; Jung, C.; Park, H. G. Illusionary" polymerase Activity Triggered by Metal Ions: Use for Molecular Logic-Gate Operations. *Angew. Chem., Int. Ed.* **2010**, *49*, 9757−9760.

(9) Petty, J. T.; Story, S. P.; Hsiang, J. C.; Dickson, R. M. DNA-Templated Molecular Silver Fluorophores. *J. Phys. Chem. Lett.* **2013**, *4*, 1148−1155.

(10) Richards, C. I.; Choi, S.; Hsiang, J.; Antoku, Y.; Vosch, T.; Bongiorno, A.; Tzeng, Y.; Dickson, R. M. Oligonucleotide-Stabilized

Ag Nanocluster Fluorophores. *J. Am. Chem. Soc.* **2008**, *130*, 5038−5039.

(11) Petty, J. T.; Sergev, O. O.; Nicholson, D. A.; Goodwin, P. M.; Giri, B.; McMullan, D. R. A Silver Cluster-DNA Equilibrium. *Anal. Chem.* **2013**, *85*, 9868−9876.

(12) O'Neill, P. R.; Gwinn, E. G.; Fygenson, D. K. UV Excitation of DNA Stabilized Ag Cluster Fluorescence via the DNA Bases. *J. Phys. Chem. C* **2011**, *115*, 24061−24066.

(13) Copp, S. M.; Schultz, D.; Swasey, S.; Pavlovich, J.; Debord, M.; Chiu, A.; Olsson, K.; Gwinn, E. Magic Numbers in DNA-Stabilized Fluorescent Silver Clusters Lead to Magic Colors. *J. Phys. Chem. Lett.* **2014**, *5*, 959−963.

(14) Ritchie, C. M.; Johnsen, K. R.; Kiser, J. R.; Antoku, Y.; Dickson, R. M.; Petty, J. T. Ag Nanocluster Formation Using a Cytosine Oligonucleotide Template. *J. Phys. Chem. C* **2007**, *111*, 175−181.

(15) Oemrawsingh, S. S. R.; Markešević, N.; Gwinn, E. G.; Eliel, E. R.; Bouwmeester, D. Spectral Properties of Individual DNA-Hosted Silver Nanoclusters at Low Temperatures. *J. Phys. Chem. C* **2012**, *116* (48), 25568−25575.

(16) Vosch, T.; Antoku, Y.; Hsiang, J.; Richards, C. I.; Gonzalez, J. I.; Dickson, R. M. Strongly Emissive Individual DNA-Encapsulated Ag Nanoclusters as Single-Molecule Fluorophores. *Proc. Natl. Acad. Sci. U. S. A.* **2007**, *104*, 12616−12621.

(17) Choi, S.; Dickson, R. M.; Yu, J. Developing Luminescent Silver Nanodots for Biological Applications. *Chem. Soc. Rev.* **2012**, *41*, 1867−1891.

(18) Díez, I.; Ras, R. H. A. Fluorescent Silver Nanoclusters. *Nanoscale* **2011**, *3*, 1963−1970.

(19) Xu, H.; Suslick, K. S. Water-Soluble Fluorescent Silver Nanoclusters. *Adv. Mater.* **2010**, *22*, 1078−1082.

(20) Guo, S.; Wang, E. Noble Metal Nanomaterials: Controllable Synthesis and Application in Fuel Cells and Analytical Sensors. *Nano Today* **2011**, *6*, 240−264.

(21) Shang, L.; Dong, S.; Nienhaus, G. U. Ultra-Small Fluorescent Metal Nanoclusters: Synthesis and Biological Applications. *Nano Today* **2011**, *6*, 401−418.

(22) Latorre, A.; Somoza, Á. DNA-Mediated Silver Nanoclusters: Synthesis, Properties and Applications. *ChemBioChem* **2012**, *13*, 951−958.

(23) Schultz, D.; Gardner, K.; Oemrawsingh, S. S. R.; Markešević, N.; Olsson, K.; Debord, M.; Bouwmeester, D.; Gwinn, E. Evidence for Rod-Shaped DNA-Stabilized Silver Nanocluster Emitters. *Adv. Mater.* **2013**, *25*, 2797−2803.

(24) Swasey, S. M.; Karimova, N.; Aikens, C. M.; Schultz, D. E.; Simon, A. J.; Gwinn, E. G. Chiral Electronic Transitions in Fluorescent Silver Clusters Stabilized by DNA. *ACS Nano* **2014**, *8*, 6883−6892.

(25) Johnson, H. E.; Aikens, C. M. Electronic Structure and TDDFT Optical Absorption Spectra of Silver Nanorods. *J. Phys. Chem. A* **2009**, *113*, 4445−4450.

(26) Karimova, N. V.; Aikens, C. M. Time-Dependent Density Functional Theory Investigation of the Electronic Structure and Chiroptical Properties of Curved and Helical Silver Nanowires. *J. Phys. Chem. A* **2015**, *119*, 8163−8173.

(27) Guidez, E. B.; Aikens, C. M. Theoretical Analysis of the Optical Excitation Spectra of Silver and Gold Nanowires. *Nanoscale* **2012**, *4*, 4190−4198.

(28) Petty, J. T.; Zheng, J.; Hud, N. V.; Dickson, R. M. DNA-Templated Ag Nanocluster Formation. *J. Am. Chem. Soc.* **2004**, *126*, 5207−5212.

(29) Berdakin, M.; Féraud, G.; Dedonder-Lardeux, C.; Jouvet, C.; Pino, G. A. Effect of Ag+ on the Excited-State Properties of a Gas-Phase (Cytosine)₂Ag+ Complex: Electronic Transition and Estimated Lifetime. *J. Phys. Chem. Lett.* **2014**, *5*, 2295−2301.

(30) Taccone, M. I.; Féraud, G.; Berdakin, M.; Dedonder-Lardeux, C.; Jouvet, C.; Pino, G. A. Communication: UV Photoionization of Cytosine Catalyzed by Ag+. *J. Chem. Phys.* **2015**, *143*, 041103.

(31) Gwinn, E.; Schultz, D.; Copp, S.; Swasey, S. DNA-Protected Silver Clusters for Nanophotonics. *Nanomaterials* **2015**, *5*, 180−207.

(32) Megger, D. a.; Müller, J. Silver(I)-Mediated Cytosine Self-Pairing Is Preferred Over Hoogsteen-Type Base Pairs with the Artificial Nucleobase 1,3-Dideaza-6-Nitropurine. *Nucleosides, Nucleotides Nucleic Acids* **2010**, *29*, 27−38.

(33) Ono, A.; Torigoe, H.; Tanaka, Y.; Okamoto, I. Binding of Metal Ions by Pyrimidine Base Pairs in DNA Duplexes. *Chem. Soc. Rev.* **2011**, *40*, 5855−5866.

(34) Urata, H.; Yamaguchi, E.; Nakamura, Y.; Wada, S. Pyrimidine-Pyrimidine Base Pairs Stabilized by silver(I) Ions. *Chem. Commun.* **2011**, *47*, 941−943.

(35) Ono, A.; Cao, S.; Togashi, H.; Tashiro, M.; Fujimoto, T.; Machinami, T.; Oda, S.; Miyake, Y.; Okamoto, I.; Tanaka, Y. Specific Interactions between silver(I) Ions and Cytosine−cytosine Pairs. *Chem. Commun.* **2008**, 4825−4827.

(36) Berdakin, M.; Steinmetz, V.; Maitre, P.; Pino, G. A. Gas Phase Structure of Metal Mediated (Cytosine)₂Ag+ Mimics the Hemiprotonated (Cytosine)₂H+ Dimer in I-Motif Folding. *J. Phys. Chem. A* **2014**, *118*, 3804−3809.

(37) Leontis, N. B.; SantaLucia, J., Eds. *Molecular Modeling of Nucleic Acids*; American Chemical Society: Washington, DC, 1997.

(38) Humphrey, W.; Dalke, A.; Schulten, K. VMD—Visual Molecular Dynamics. *J. Mol. Graphics* **1996**, *14*, 33−38.

(39) Plimpton, S. Fast Parallel Algorithms for Short-Range Molecular Dynamics. *J. Comput. Phys.* **1995**, *117*, 1−19.

(40) Foloppe, N.; MacKerell, A. D., Jr. All-Atom Empirical Force Field for Nucleic Acids: I. Parameter Optimization Based on Small Molecule and Condensed Phase Macromolecular Target Data. *J. Comput. Chem.* **2000**, *21*, 86−104.

(41) MacKerell, A. D.; Banavali, N. K. All-Atom Empirical Force Field for Nucleic Acids: II. Application to Molecular Dynamics Simulations of DNA and RNA in Solution. *J. Comput. Chem.* **2000**, *21*, 105−120.

(42) Wu, D. Y.; Hayashi, M.; Shiu, Y. J.; Liang, K. K.; Chang, C. H.; Yeh, Y. L.; Lin, S. H. A Quantum Chemical Study of Bonding Interaction, Vibrational Frequencies, Force Constants, and Vibrational Coupling of Pyridine−Mₙ (M = Cu, Ag, Au; N = 2−4). *J. Phys. Chem. A* **2003**, *107*, 9658−9667.

(43) Lin, F.; Wang, R. Systematic Derivation of AMBER Force Field Parameters Applicable to Zinc-Containing Systems. *J. Chem. Theory Comput.* **2010**, *6*, 1852−1870.

(44) Staelens, N.; Leherte, L.; Champagne, B.; Vercauteren, D. P. Modeling of Structural, Energetic, and Dynamic Properties of Few-Atom Silver Clusters Embedded in Polynucleotide Strands by Using Molecular Dynamics. *ChemPhysChem* **2015**, *16* (2), 360−369.

(45) Negre, C. F. A.; Fuertes, V. C.; Oviedo, M. B.; Oliva, F. Y.; Sánchez, C. G. Quantum Dynamics of Light-Induced Charge Injection in a Model Dye−Nanoparticle Complex. *J. Phys. Chem. C* **2012**, *116* (28), 14748−14753.

(46) Oviedo, M. B.; Negre, C. F. A.; Sanchez, C. G. Dynamical Simulation of the Optical Response of Photosynthetic Pigments. *Phys. Chem. Chem. Phys.* **2010**, *12* (25), 6706−6711.

(47) Oviedo, M. B.; Sánchez, C. G. Transition Dipole Moments of the Qy Band in Photosynthetic Pigments. *J. Phys. Chem. A* **2011**, *115*, 12280−12285.

(48) Elstner, M.; Porezag, D.; Jungnickel, G.; Elsner, J.; Haugk, M.; Frauenheim, T.; Suhai, S.; Seifert, G. Self-Consistent-Charge Density-Functional Tight-Binding Method for Simulations of Complex Materials Properties. *Phys. Rev. B: Condens. Matter Mater. Phys.* **1998**, *58*, 7260−7268.

(49) Aradi, B.; Hourahine, B.; Frauenheim, T. DFTB+, A Sparse Matrix-Based Implementation of the DFTB Method. *J. Phys. Chem. A* **2007**, *111*, 5678−5684.

(50) Gaus, M.; Cui, Q.; Elstner, M. DFTB3: Extension of the Self-Consistent-Charge Density-Functional Tight-Binding Method (SCC-DFTB). *J. Chem. Theory Comput.* **2011**, *7*, 931−948.

(51) Oviedo, M. B.; Zarate, X.; Negre, C. F. A.; Schott, E.; Arratia-Pérez, R.; Sánchez, C. G. Quantum Dynamical Simulations as a Tool for Predicting Photoinjection Mechanisms in Dye-Sensitized TiO2 Solar Cells. *J. Phys. Chem. Lett.* **2012**, *3*, 2548−2555.

(52) Negre, C. F. A.; Young, K. J.; Oviedo, Ma. B.; Allen, L. J.; Sanchez, C. G.; Jarzembska, K. N.; Benedict, J. B.; Crabtree, R. H.; Coppens, P.; Brudvig, G. W.; et al. Photoelectrochemical Hole Injection Revealed in Polyoxotitanate Nanocrystals Functionalized with Organic Adsorbates. *J. Am. Chem. Soc.* **2014**, *136*, 16420−16429.

(53) Fleig, T.; Knecht, S.; Hättig, C. Quantum-Chemical Investigation of the Structures and Electronic Spectra of the Nucleic Acid Bases at the Coupled Cluster CC2 Level. *J. Phys. Chem. A* **2007**, *111*, 5482−5491.

(54) Varsano, D.; Di Felice, R.; Marques, M. A. L.; Rubio, A. A TDDFT Study of the Excited States of DNA Bases and Their Assemblies. *J. Phys. Chem. B* **2006**, *110*, 7129−7138.

(55) Gwinn, E.; Schultz, D.; Copp, S.; Swasey, S. DNA-Protected Silver Clusters for Nanophotonics. *Nanomaterials* **2015**, *5*, 180−207.

H